Sorption hysteresis on soils and sediments: obtaining characteristic free energies using "single-point desorption isotherms"

Running head: *Sorption hysteresis-characteristic free energies*

Mikhail Borisover*

Agricultural Research Organization, Institute of Soil, Water and Environmental Sciences, The Volcani Center, Rishon LeZion, P.O. Box 15159, 7505101, Israel

*Corresponding author. E-mail address: vwmichel@volcani.agri.gov.il; telephone: 972-3-9683314; fax: 972-3-9604017. Mailing address: Agricultural Research Organization, Institute of Soil, Water and Environmental Sciences, The Volcani Center, P.O. Box 15159, Rishon LeZion 7505101, Israel.

Summary

Sorption-desorption hysteresis (SDH) may control distributions of chemicals between diverse environmental phases, including soils and sediments. Formation of metastable states caused by pore deformation or inelastic swelling of a sorbent and their persistence during desorption were considered in the literature as one reason for "true" SDH. Such metastable states persisting during desorption lead to the lack of closure of sorption-desorption loop at non-zero sorbate concentrations, which is often observed in soil and environmental literature. Also, SDH was often characterized using single-point desorption isotherms (DIs) combining sorbed states reached during single desorption steps started from different points along a sorption isotherm (SI). The objective of this contribution is to demonstrate how the single-point DIs could be used to characterize SDH in liquid phase sorption experiments in terms of Gibbs free energy. This free energy is accumulated in some non-relaxed sorbed states belonging to DI as compared with the states of the same composition (sorbed concentration) belonging to SI. Using the literature data on SIs and single-point DIs of some polycyclic aromatic hydrocarbons and pesticides on soils and sediments, it is shown how these extra free energies could be obtained and how they could change in the selected sorbate-sorbent systems. When the extent of SDH decreases with increasing solute concentration, these additional free energies decline. They may remain constant or even increase, suggesting in the latter case that a larger work is needed to perturb a sorbent structure at higher sorbed concentrations. This paper proposes a novel approach for quantifying and understanding liquid phase SDH in the cases when a thermodynamic justification is sought, and, therefore, it advances the ability to predict the fate and activity of multiple chemicals in typical soil/sediment environments.

Keywords: sorption, desorption, hysteresis, "frozen" state, metastable state, free energy, natural organic matter, clay, organic sorbate, liquid phase

Highlights

- Desorption from soils and sediments to solutions may be hysteretic due to formed metastable states
- Hysteresis is quantified in terms of excessive free energies of metastable states
- Extra free energies are sorbate- and sorbent-dependent, varying across sorption isotherms
- Single-point desorption isotherms allow to determine free energy excess of metastable states

Introduction

Examination of sorption of multiple chemicals on soils and sediments is clearly recognized to be essential for understanding and prediction of environmental distribution, fate and bioavailability of chemicals (OECD 106, 2000). When obtaining sorption-desorption data relating concentrations of a chemical in a sorbed phase to its concentration in an external phase (i.e., solution or gas), hysteresis may often make itself evident in non-coinciding sorption and desorption isotherms (SI and DI, respectively). Such a sorption-desorption hysteresis (SDH) is known to appear even when the artifacts, e.g., biodegradation, a loss of sorbing and sorbed materials, changes in solvents, non-accounted sorption/desorption kinetics, seem to be ruled out. In relation to liquid-phase sorption of non-ionized organic chemicals on soil (natural) organic matter (OM), one concept explaining SDH links sorption irreversibility to metastable states formed in a sorption-desorption sequence such that those states being at local incomplete equilibria and associated with free exchange of solute and solvent molecules persist across DI (Sander et al., 2005; Sander & Pignatello, 2009; Cao et al., 2016). Importantly, when these metastable states persist, there is no closure of sorption-desorption loop at non-zero concentrations of sorbates that is the often case in soil sorption experiments.

In liquid phase experiments, desorption data is often obtained by remove/refill method. This method involves removing a precise part of a solution volume, in the end of sorption experiment, and replacing it with the same volume of a solvent. This added solvent volume does not contain a solute of interest but it is supposed to be maintained at the same pH, ionic composition and whole solution chemistry including potential presence of dissolved OM as in the solution phase in sorption experiments. In this way, the reduced solute concentration triggers desorption. By reaching an (apparent) desorption equilibrium and consecutively

replacing the solution phase with a next new solvent portion, the successive DI is obtained such that each "point" across this DI shares the same initial history associated with the SI point at which desorption started. Less aggressive way to obtain a DI which does not involve phase separation and centrifugation may involve a direct dilution of a system with increasing the solution volume (Altfelder et al., 2000; Bowman & Sans, 1985). In this way, no any portion of a solution is removed, but the solvent portion added to reduce solute concentration initiates desorption.

Recently, an approach was proposed to quantify SDH explained by formation of metastable states and their persistence across successive desorption in terms of the Gibbs free energy accumulated due to non-relaxed changes in a sorbed state (Borisover, 2019). This approach requested integration of sorbed concentrations over properly transformed SI followed with integration over successive DI and may be applied to different types of sorbing materials, not necessarily soil OM. As distinct of multiple empirical indices used for characterizing SDH (e.g., reviewed by Sander et al., 2005), the obtained thermodynamic quantities directly show how a sorbed state formed in the end of successive desorption is far from that one equivalent in terms of a chemical composition but belonging to SI. Therefore, relations between these free energy values, chemical structure of sorbates, composition and physico-chemical properties of sorbents and various intermolecular interactions in a sorbed state may be sought thus improving our understanding of SDH mechanisms.

The approach described earlier (Borisover, 2019) was focused on using successive DIs. However, besides obtaining successive DIs, in multiple studies desorption has been examined with the single-step remove/refill started at different initial sorbed concentrations across SI (Zhang et al., 2010ab, 2014; Martins et al., 2018; Mosquera-Vivas et al., 2016; Piwowarczyk

& Holden, 2012; Gaonkar et al., 2019; Kandil et al., 2015; Kin et al. 2003; Ran et al., 2002 and many others). Then, the determined sorbed concentrations are combined in one curve also called DI ("single-point" or sometimes "single step" DI).

The single-point DIs in liquid phase sorption experiments were considered thermodynamically flawed (Bowman & Sans, 1985; Sander et al., 2005) since the different states across the DI line do not share the same history of sorption and represent rather an "artificial" trend that cannot be treated thermodynamically. Yet, as mentioned above, such single-point DIs are widely used in soil and environmental sorption literature. At least one reason to obtain such single-point desorption data is that by this way an extent of sorption-desorption irreversibility may be easily examined and empirically quantified at multiple concentrations of solute/sorbate albeit only in one desorption step. When SDH is thought to be related to formation of metastable sorbed states, each single desorption point when combined in one " isotherm" trend encompasses valuable information on how the sorbent perturbed during sorption resists relaxation along desorption thus accumulating additional free energy, and how this extra free energy changes across a range of sorbed concentrations. The objective of this contribution is to demonstrate how the single-point DIs data may be used to characterize SDH observed in liquid phase sorption experiments in terms of free energy of non-relaxed states.

Methodology

Theoretical background

In the two-phase system containing, at given temperature and pressure, three components, i.e., a sorbent (S), solvent and a sorbing compound of interest (A), SDH has been expressed in terms of the Gibbs free energy quantities (Borisover, 2019). This quantification was proposed for the

SDH caused by newly formed and persisting metastable states and, therefore, showing no loop closure at non-zero solute concentrations. Hence, it is presumed that no return to the fully equilibrated state is observed in experimental timeframe during desorption. Briefly, for sorption (1→2) - desorption (2→3) sequence (Fig. 1a; Points 1 and 3 are characterized with the same sorbed concentration), extra Gibbs free energy (ΔG^{ext}) is accumulated at Point 3, as compared with Point 1, due to the formed and persisting metastable states.

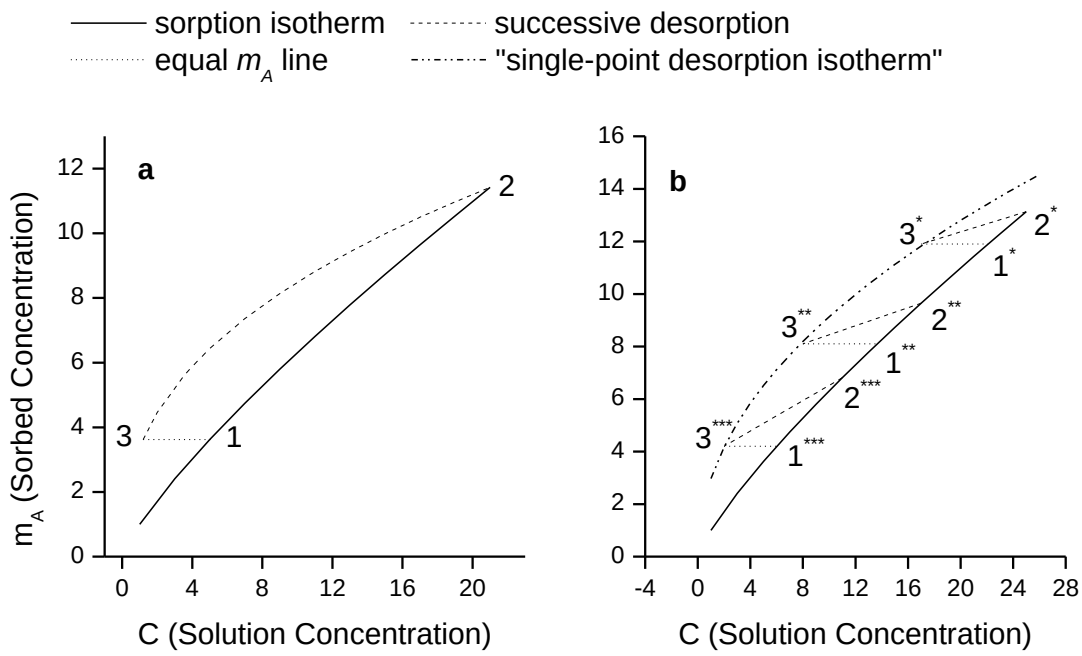

Figure 1. Sorbed concentrations (i.e., sorbate mole amounts m_A per unit sorbent mass) plotted against solution concentration C. (a) The solid 1→2 line and the dashed 2→3 line depict SI and DI, respectively. The 1→3 line connects equal sorbed concentrations. (b) Each solid line element connecting the states associated with the similarly marked Points 1 and 2 (having the same number of stars) belongs to SI. The dashed lines connecting similarly marked Points 2 and 3 represent a single step of desorption. The dash dot dot line connecting all the Points 3, regardless to marking, represents "a single-point DI". The 1→3 line of any type connects equal sorbed concentrations.

This additional Gibbs free energy ΔG^{ext} quantifying the extent of hysteresis is obtained by integration of $\Delta\mu_A$ over SI (1→2) and DI (2→3) paths (Eqn. 1) where $\Delta\mu_A$ is the change of chemical potential of sorbing component A during its transfer from a hypothetical reference state in an infinitely diluted solution at unit concentration to an actual sorbed state.

$$\Delta G^{ext} = \Delta G_{1\to2\to3} = \int_1^2 \Delta\mu_A dm_A + \int_2^3 \Delta\mu_A dm_A \quad (1)$$

m_A is the sorbate mole amount per unit sorbent mass (i.e., sorbed concentration of component A). Sorbate and solvent molecules are presumed *to freely exchange between sorbed states belonging to SI and DI and an external liquid phase* such that for each exchangeable component its chemical potentials in both coexisting phases tend to be equal. For sorption of non-ionized solute A from the sufficiently diluted liquid phase equilibrated with a sorbent, $\Delta\mu_A$ is obtained from solution concentration C of component A in an equilibrated solution:

$$\Delta\mu_A = \mu_A - \mu_A^0 = RTlnC \quad (2)$$

where μ_A is the chemical potential of sorbing compound A in a whole system, μ_A^0 is its chemical potential in the hypothetical reference state in an infinitely diluted solution at unit concentration, and R and T are the universal gas constant and absolute temperature (in Kelvin), respectively. Therefore,

$$\Delta G^{ext} = RT\left(\int_1^2 lnCdm_A + \int_2^3 lnCdm_A\right) \quad (3)$$

Changes in sorbent S caused by increase in the sorbed concentration of component A are expected to be foremost responsible for appearance of SDH (Lu & Pignatello, 2002; Sander & Pignatello, 2009; Cao et al., 2016). Using the Gibbs-Duhem relationship, the sorbent S-associated contribution ΔG_S^{ext} to the total extra Gibbs free energy ΔG^{ext} is obtained as the following (Borisover, 2019):

$$\Delta G_S^{ext} = -RT\left(\int_1^2 m_A\, dlnC + \int_2^3 m_A\, dlnC\right) \quad (4)$$

Since it is the ($m_{A,2} - m_{A,1}$) rise in sorbed concentrations (Fig. 1a) which caused perturbations in sorbent S and eventually led to SDH, a molar value $\widetilde{\Delta G}_S^{ext}$ has been introduced by normalizing ΔG_S^{ext} to the difference ($m_{A,2} - m_{A,1}$) (Eqn. 5).

$$\widetilde{\Delta G}_S^{ext} = \frac{\Delta G_S^{ext}}{m_{A,2} - m_{A,1}} = -RT\,\frac{\int_1^2 m_A dlnC + \int_2^3 m_A dlnC}{m_{A,2} - m_{A,1}} \quad (5)$$

The obtained $\widetilde{\Delta G}_S^{ext}$ quantity represents a work needed to generate metastable sorbed states and averaged over the sorbed concentration range. Dividing $\widetilde{\Delta G}_S^{ext}$ by RT produced a unitless integral hysteresis index (*IHI*; Borisover, 2019).

One examined case (Borisover, 2019) involved the SI approximated by Freundlich model (Eqn. 6) whereas the successive DI is described with the Freundlich-model expression amended with an empirical constant *d* (Eqn. 7):

$$m_A = K_{F,SI} C^{n_{SI}} \quad (6)$$

$$m_A = d + K_{F,DI} C^{n_{DI}} \quad (7)$$

where the subscripts and the superscripts SI and DI refer to the parameters of the model applied to either SI or DI. The *d* constant was introduced to indicate that experimental DIs might obey a trend with an apparently non-zero intercept at the y (sorbed concentration) -axis. Since formation of non-exchangeable (non-desorbing) fractions of chemicals is not in the focus of the earlier and current analysis, Eqn. (7) cannot be straightforwardly extrapolated to zero solute concentration. For these particular types of SI and DI (Eqns. 6, 7) the molar $\widetilde{\Delta G}_S^{ext}$ was obtained as the following (Borisover, 2019):

$$\widetilde{\Delta G}_S^{ext} = RT\left(\frac{1}{n_{DI}} - \frac{1}{n_{SI}} - \frac{d}{n_{DI}(m_{A,2}-m_{A,1})} ln\frac{m_{A,1}-d}{m_{A,2}-d}\right) \quad (8)$$

In the current analysis, the desorptions are made as the single steps from different Points 2 across SI (Fig. 1b) such that eventually a "single-point DI" is formed by connecting the final states (Points 3) reached in multiple desorptions. Each single desorption is represented by a straight line, with n_{DI}=1, connecting similarly marked Points 2 and 3 (Fig. 1b). Therefore, the expression for $\widetilde{\Delta G}_S^{ext}$ (Eqn. 8) is transformed into Eqn. (9):

$$\widetilde{\Delta G}_S^{ext} = RT\left(1 - \frac{1}{n_{SI}} - \frac{d}{m_{A,2}-m_{A,1}} ln\frac{m_{A,1}-d}{m_{A,2}-d}\right) \quad (9)$$

Calculating free energy values using available "single-point desorption isotherm" data

In calculating the $\widetilde{\Delta G}_S^{ext}$ values with Eqn. (9), $m_{A,1}$ is the sorbed concentration at which sorption sequence started (any Point 1 in Fig. 1b) and $m_{A,2}$ represents the sorbed concentration belonging to SI, at which desorption started (any Point 2 in Fig. 1b). Finally, $m_{A,1}$ was also reached after one desorption step at Point 3 (Fig. 1b; $m_{A,3}$=$m_{A,1}$). This resulting sorbed concentration at any Point 3 ($m_{A,1}$) is decreased by x as compared with that ($m_{A,2}$) attained during sorption (Fig. 1b). The further mass balance associated with one-step desorption is as the following: a (1-α) fraction of supernatant solution is replaced during desorption with a solute-free liquid phase contacting with a sorbent in a volume to mass ratio as such as one to r. Respectively, the solution concentration C_3 is changed as compared with C_2:

$$C_3 = C_2 \propto +rx \quad (10)$$

In a set of Points 3 (marked with different number of stars in Fig. 1b), sorbed and solution concentrations are in the Freundlich model-like connection representing a single-point DI:

$$(m_{A,2} - x) = k_F(C_2 \propto +rx)^n \quad (11)$$

where k_F and n are the parameters of this single-point DI.

Hence, using $K_{F,SI}$, n_{SI} and Eqn. (6), sorbed concentration $m_{A,2}$ belonging to SI is calculated for any selected C_2. Further, with the known k_F, n, α and r parameters, the decrease x during desorption is recovered with Eqn. (11), thus producing $m_{A,3}$ (=$m_{A,1}$) and, with Eqn. (10), C_3. The solving Eqn. (11) was performed using the Excel Solver. Having the sorbed and solution concentrations at various Points 2 and 3 (Fig. 1b), the intercept d of the straight-line connecting different pairs of Points 2 and 3 is calculated. Thus, the $\widetilde{\Delta G}_S^{ext}$ values may be computed for each solution/sorbed concentration of interest, using Eqn. (9).

Data analysis and discussion

In further analysis, the sorption-desorption data from several literature studies were used. The selected examples were those in which chemical transformations, biodegradation of chemicals or their speciation were excluded or not considered by authors as significant. In addition, the studies in which slow sorption/desorption kinetics were explicitly demonstrated, are avoided. The examples brought in the current analysis serve, foremost, the goal to demonstrate the approach how single-point DIs may elucidate Gibbs free energies of formation of metastable states when the latter could be seen as a cause for sorption-desorption hysteresis. This analysis is not suitable for the data demonstrating sorbate entrapment in the sorbent matrix not allowing molecules to freely participate in partitioning equilibria.

Free energies associated with SDH of polycyclic aromatic hydrocarbons on a soil and a sediment

Wu and Sun (2010) obtained the sorption-desorption data for phenanthrene on a soil in aqueous solutions at the presence of biocide, sodium azide, in the 48 hrs equilibration, such that the kinetics tests were performed in the period from 10 min to 120 hrs and demonstrated that the apparent equilibrium was reached after 24 hrs. Fig. 2a shows the sorption-desorption data simulated using the reported parameters of SI and single-point DI (Wu and Sun, 2010) in the concentration range studied. Phenanthrene as many other aromatic hydrocarbons is well recognized to interact with soil OM as its major sorption domain when soil is fully hydrated. Then, using the above-described procedure (Section 2.2), the $\widetilde{\Delta G_S^{ext}}$ values were computed for a series of the SI solution concentrations representing different Points 2 (as in Fig. 1) at which single steps of desorption were started. Finally, the $\widetilde{\Delta G_S^{ext}}$ values are plotted in Fig. 2a against these solution concentrations.

The obtained free energy values are positive thus indicating that a work has to be made in order to create the state associated with Point 3 from the state assigned to Point 1 (Fig. 2a) despite both states are characterized by the same sorbed concentration. Such a work upon the creation of the metastable sorbed state (in consideration that this mechanism is solely responsible for SDH) should most probably reflect a sorbent perturbation. The perturbation may be seen as an inelastic swelling or pore deformation of soil OM (Braida et al., 2003; Sander et al., 2005; Cao et al., 2016) or as disruption of multiple non-covalent linkages present in soil OM phase (Borisover & Graber, 2002; Borisover et al., 2011) such that these mechanisms may become not necessarily distinguishable (Graber et al., 2007). This molar work is larger at lower

solution concentrations thus proposing that a sorbed state (a sorbent) is more resistive to such perturbations when the concentration of "perturbing agent", i, e., the sorbate loading, is lower.

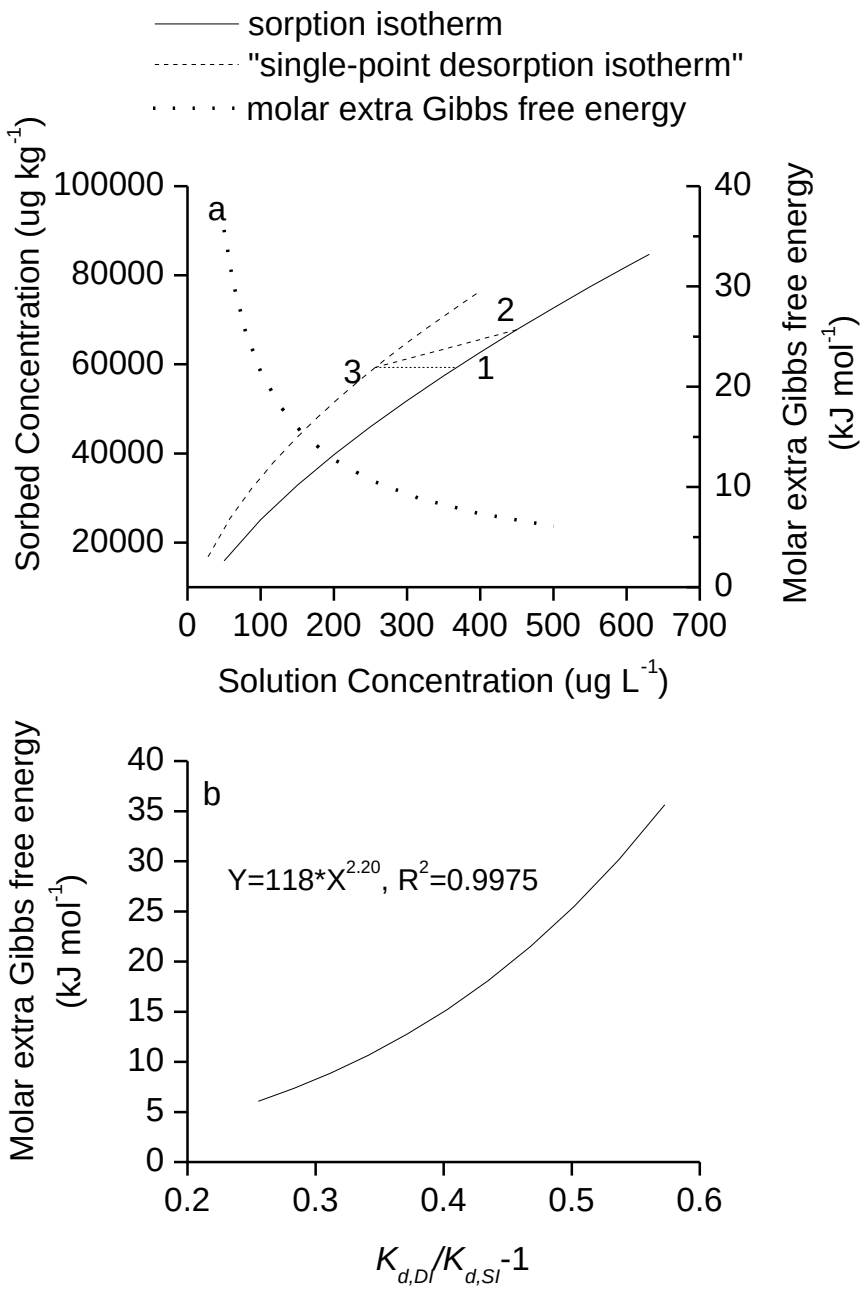

Figure 2. Sorption-desorption hysteresis of phenanthrene on a soil in aqueous solutions (simulated using the published parameters; Wu and Sun, 2010). (a) Sorption and single-point desorption isotherms refer to the left Y-axis and show sorbed concentrations vs. solution

concentrations. The explanation of Points 1,2 and 3 is provided in Fig. 1. Molar extra Gibbs free energies associated with formation of metastable states refer to the right Y-axis. They are plotted against solution concentration from which desorption started. (b) Molar extra Gibbs free energy is plotted against the empirical measure of SDH defined as $K_{d,DI}/K_{d,SI}$ -1 where the distribution coefficients $K_{d,DI}$ and $K_{d,SI}$ are associated with DI and SI, respectively, and refer to a certain common solution concentration. This concentration is associated with that of Point 3 in the notation of Fig. 1 and Fig. 2a.

One widely used way to characterize SDH considers the difference of sorbed concentrations determined for DI and SI, i.e., $m_{A,DI}$-$m_{A,SI}$, at a certain common solution concentration C, and normalized by the SI sorbed concentration (Huang et al., 1998; He at al., 2006; Zhang et al., 2018). Such a normalized ratio is related to the ratio of distribution coefficients K_d associated with SI and DI (Eqn. 12):

$$\frac{m_{A,DI}-m_{A,SI}}{m_{A,SI}} = \frac{\frac{m_{A,DI}}{C}}{\frac{m_{A,SI}}{C}} - 1 = \frac{K_{d,DI}}{K_{d,SI}} - 1 \qquad (12)$$

Based on the data by Wu and Sun (2010), the computed values of the molar $\widetilde{\Delta G}_S^{ext}$ values associated with SDH at a certain point of DI are plotted in Fig. 2b against the empirical measure of SDH obtained as $K_{d,DI}/K_{d,SI}$ -1, for the same point of DI. It is seen from Fig. 2b that the molar $\widetilde{\Delta G}_S^{ext}$ values are well connected with that empirical measure of SDH. However, the connection is non-linear and follows the power function with the exponent exceeding one. One result of such a non-linearity is that generally both measures cannot be used interchangeably: they quantify differently the relative changes of the extent of SDH across sorbed concentration range such that the molar $\widetilde{\Delta G}_S^{ext}$ values demonstrate a greater sensitivity to the concentration changes.

Oh et al. (2013) published the sorption and desorption data for three polycyclic aromatic hydrocarbons (PAHs), naphthalene, phenanthrene and pyrene, on a coastal sediment from water

of different salinity including non-saline water, providing 48 hrs for equilibration. SIs and single-point DIs were found linear regarding the plots of sorbed concentrations against solution concentrations. Using the reported parameters of the linear equations, the SIs and DIs from water were simulated and are shown in Fig. 3 for three PAHs as log sorbed concentrations against log solution concentrations.

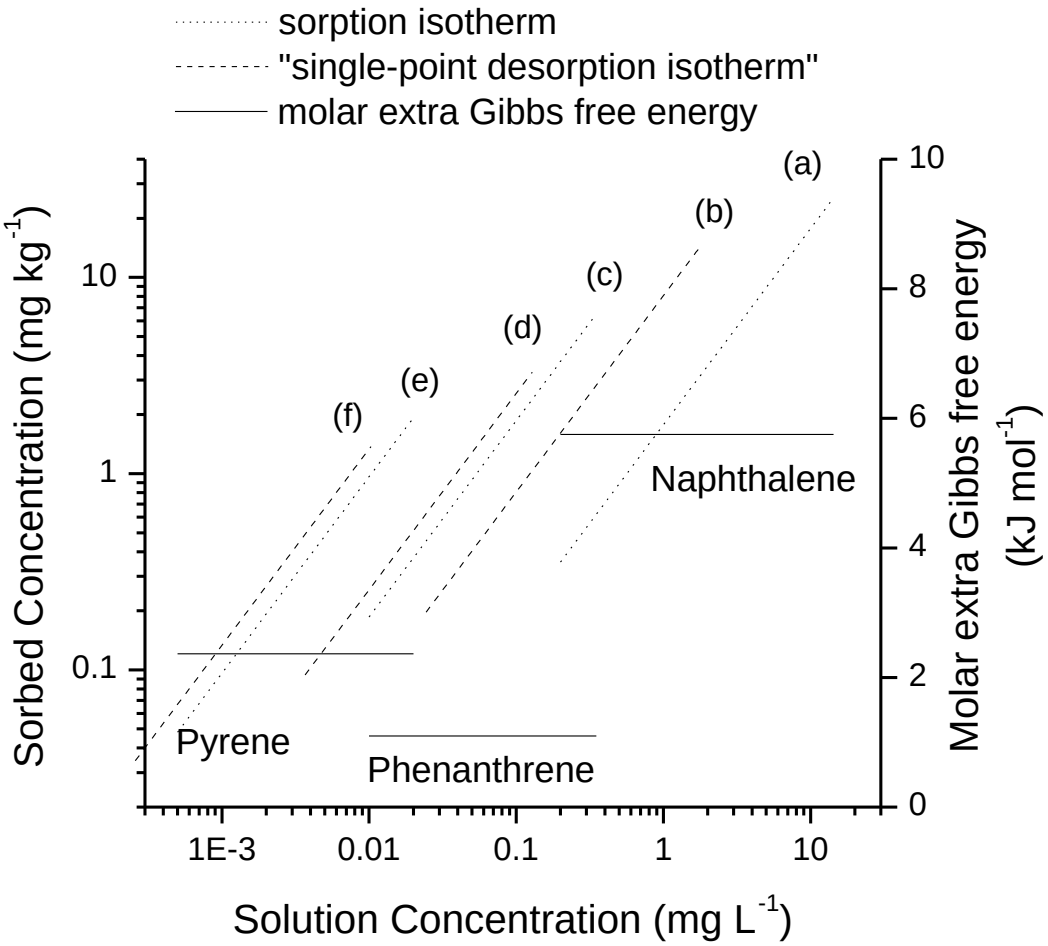

Figure 3. Sorption-desorption hysteresis of naphthalene, phenanthrene and pyrene on a coastal sediment in aqueous solutions (simulated using the published parameters; Oh et al., 2013). Sorption (a, c, e) and single-point desorption (b, d, f) isotherms refer to the left Y-axis and show log sorbed concentrations vs. log solution concentrations for naphthalene, phenanthrene and

pyrene, respectively. Molar extra Gibbs free energies associated with formation of metastable states are plotted against solution concentration from which desorption started; they are shown as horizontal lines and refer to the right Y-axis.

Since SIs and single-point DIs are linear, in the log log scale they appear as the parallel lines with the unit slope. Then, the $\widetilde{\Delta G}_S^{ext}$ values were computed for each compound and plotted against solution concentration at which single desorption steps started (Fig. 3). Due to the linearity of SIs and DIs, the calculated $\widetilde{\Delta G}_S^{ext}$ values for a given sorbate become independent on a specific solution concentration. All these values are positive with the largest values observed for naphthalene thus quantifying a strongest extent of SDH for this sorbate. By calculating the $\widetilde{\Delta G}_S^{ext}$ values of naphthalene and phenanthrene on peat and leonardite OM (Borisover, 2019), it was suggested that a larger work is required for the sorbent modification and intra-OM penetration of a larger molecule, i.e., phenanthrene. Yet, it is not so for PAH sorption-desorption on coastal sediment (Fig. 3) which may be understood that larger PAHs may not undergo intra-OM sorption but rather become associated with the OM surface thus involving lesser extents of sorbent perturbation and the SDH-linked free energies of formation of metastable states.

Free energies associated with SDH: different soil fractions and soils

Kandil et al. (2015) examined sorption and desorption of imidacloprid, a neonicotinoid insecticide, on lacustrine soil and its humic acid and clay fractions. With the pK_a values of 1.56 and 11.12 (HSDB, Toxnet, 2019), imidacloprid is practically non-ionizable in soil solutions. In the kinetics tests ranging from 15 min to 48 hrs, the equilibration time was established, and SIs

as well as single-point DIs were obtained after 24 hrs such that biodegradation, based on the reported half-life times, was considered minimal. Hence, the molar extra Gibbs free energy values $\widetilde{\Delta G_S^{ext}}$ associated with SDH were computed, using the parameters of the reported SIs and DIs as well as the solid to solution ratios used, and plotted in Fig. 4 against imidacloprid concentration in equilibrated solutions from which desorption started.

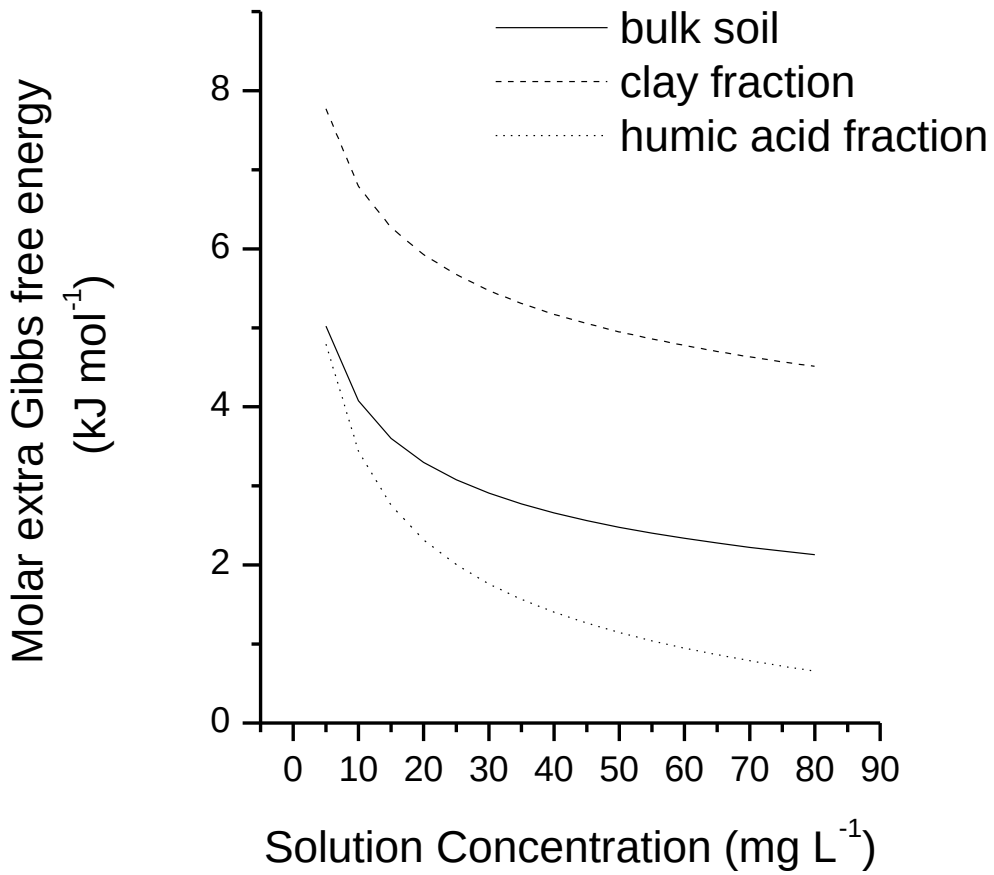

Figure 4. Molar extra Gibbs free energy associated with SDH and obtained from the single-point DIs for imidacloprid on the bulk soil and its clay and humic acid fractions (Kandil et al., 2015) plotted against compound concentration in the equilibrated solutions from which desorption started.

On all the three materials, the $\widetilde{\Delta G}_S^{ext}$values are positive and decline with increasing solution concentration thus exhibiting how the work to create the SDH-responsible metastable states tends to disappear at higher concentrations of imidacloprid. At a given solution concentration the $\widetilde{\Delta G}_S^{ext}$values on three sorbents are in the following order: humic acid fraction < bulk soil < clay fraction albeit the difference between humic acid fraction and bulk soil becomes negligible at lower solute concentrations (Fig. 4).

The larger $\widetilde{\Delta G}_S^{ext}$values on the clay fraction as compared with the humic acid fraction may be related to more rigid aluminosilicate nature of clay aggregates as compared with the humic acid fraction composed of generally flexible fragments of OM. The OM may be expected to undergo a better relaxation of perturbed sorption sites/OM moieties during desorption such that less work is required to alter a sorbent and accommodate a sorbate molecule in a state belonging to DI as compared with the SI state of the same composition. The soil sorbent including both fractions is expectedly found in-between the clay and humic acid fractions. Importantly, in terms of the free energy that could be accumulated in the metastable states formed and persisting during desorption, humic acid fraction seems to control soil SDH at lower solute concentrations. It is despite in the original work the major role of clay minerals in imidacloprid sorption by soil was proposed (Kandil et al, 2015). However, indeed with increasing solute concentration, the parallelism between the $\widetilde{\Delta G}_S^{ext}$values associated with the bulk soil and the clay fraction is better expressed as compared with that between the soil and the humic acid fraction. This may be proved by examining linear regressions of the $\widetilde{\Delta G}_S^{ext}$values on the clay and humic acid fractions upon that of the bulk soil. In the both cases, the correlation coefficients exceeded 0.999. However, when linking the clay fraction and the bulk soil, the slope in the regression equation is distinctly more close to one, i.e., 1.14±0.01 (with the standard

error as a statistics measure) as compared with that of the humic acid fraction vs the bulk soil (the slope of the linear association between the relevant $\widetilde{\Delta G}_S^{ext}$values is 1.43±0.001). On this soil, the SDH control dominated at lower solute concentrations by the humic acid fraction becomes more influenced by the clay fraction at higher imidacloprid concentrations.

Chen et al. (2018) examined the behavior of bidirectional systemic insecticide, spirotetramat, in a series of soils in sorption-desorption experiments. In the soils studied, pH of soil solutions varied between 4.4 and 8.2 such that this insecticide characterized with pK 10.7 (Fischer & Weiss, 2008; Jeschke, 2016) did not ionize in solutions. Sorption tests had been performed at the presence of sodium azide, with the time varied from 2 to 48 hrs, such that the 24 hrs equilibration period was allowed for both measuring SIs and single-point DIs. The free energy values $\widetilde{\Delta G}_S^{ext}$ calculated for this insecticide on some soils studied are plotted in Fig. 5 against solution concentration corresponding to an apparent sorption equilibrium from which desorption started (formally representing Points 2 in Fig. 2b). The calculation procedure is that one described in section 2.2.

As it is seen in Fig. 5, the loam soil is characterized by significant positive $\widetilde{\Delta G}_S^{ext}$ values decreasing when solution concentration increases. In opposite, the positive $\widetilde{\Delta G}_S^{ext}$ values related to the clay loam slightly increase with solution concentration, as well as the values related to the clay. In the latter case, the $\widetilde{\Delta G}_S^{ext}$ values are even slightly negative at lower solute concentrations, which indicates that DI was positioned here below the SI due most probably to a lack of SDH in this region. For these three selected soils, the $\widetilde{\Delta G}_S^{ext}$ values increase in the following order: clay < clay loam < loam whereas the clay content and the soil pH decrease in the same series (Chen et al., 2018).

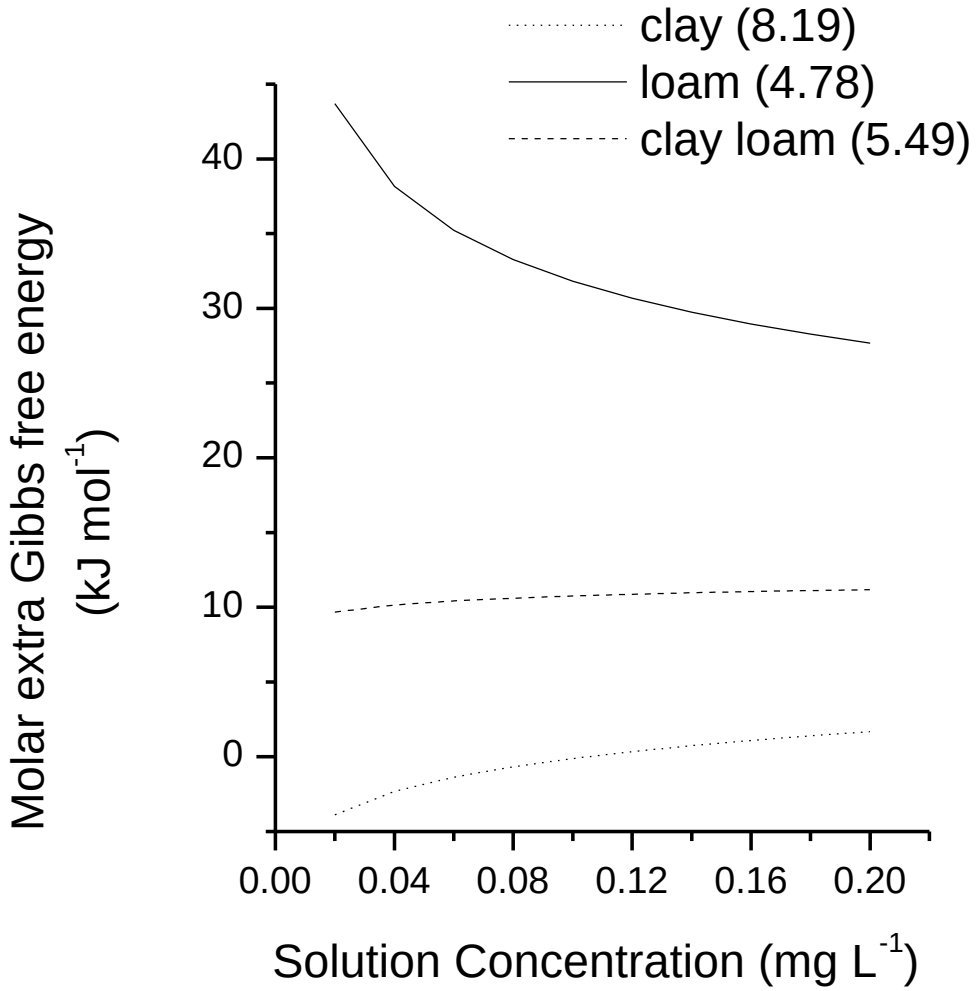

Figure 5. Molar extra Gibbs free energy associated with SDH and obtained from the single-point DIs for spirotetramat on the three soils (Chen et al., 2018) plotted against compound concentration in the equilibrated solutions from which desorption started. The values in the legend indicate the soil pH.

Obviously, multiple factors may result to the above differences in the $\widetilde{\Delta G}_S^{ext}$ values, and it is not the aim of this contribution to reexamine the original publication. However, it should be kept in mind that the lowered pH involves a shift of the dissociation equilibria of the soil

OM carboxylic groups to the protonated forms. The pK values of strongly acidic groups of humic substances may vary in the 2-5.5 range (Leenher et al., 2003), and the multiple extracted humic substances showed this protonation/ionization range even more narrow, i.e., between 3.5 and 4.6 (IHSS, Acidic Functional Groups of IHSS Samples, 2019). Therefore, such a pH shift in the loam OM may be associated with rise in the number and strength of H-bonds formed with non-ionized carboxylic groups in the soil OM phase. This may enrich soil OM with non-covalent linkages thus requiring a greater work for perturbing a sorbent, disrupting multiple interactions, incorporating and accommodating the sorbate molecules in the soil OM phase. A relaxation/re-binding of disrupted interactions in soil OM during desorption may become essentially incomplete thus leading to greater extents of SDH and larger $\widetilde{\Delta G_S^{ext}}$ values. Also, in the original work (Chen et al., 2018), structural soil changes induced by pH were mentioned as a factor influencing compound-soil interactions.

Conclusions

Creation of metastable states in a sorbent during sorption-desorption sequence and their persistence during desorption was indicated earlier in the literature as one mechanism leading to so-called "true" hysteresis on soils and sediments in liquid phase sorption experiments. In this scenario, sorption-desorption loop is not closed at non-zero concentrations of a sorbing chemical, which is an often case in sorption of organic compounds by soils and sediments from solutions. If so, such newly formed metastable states can be characterized by additional free energy as compared with the states of the same composition, i.e., the same sorbed concentration, belonging to sorption isotherms. It is demonstrated that this additional free energy may be computed using so-called "singe-point desorption isotherms" composed of the states reached

through multiple independent single desorptions started from different points along sorption isotherm. Obtained additional, extra free energies represent a variety of physico-chemical features of the sorbate/sorbent/solvent systems, being dependent on the sorbate structure, sorbed concentration range and the sorbent nature. So, the extra free energies may decline with increasing solute concentration, thus indicating lesser extents of hysteresis. They may remain constant or even increase, suggesting that in the last case at higher sorbed concentrations of chemicals a larger work is needed to perturb a sorbent structure and create a sorbed state belonging to DI as compared with the same composition state belonging to SI. Obtaining such free energy quantities suggests a basis for thermodynamic examination of multiple cases of sorption-desorption hysteresis found on soils and sediments that may be linked to formation of metastable states.

Declarations of interest: none

The data that support the findings of this study are available from the corresponding author upon reasonable request.

References

Altfelder, S., Streck, T. & Richter, J. (2000). Nonsingular sorption of organic compounds in soil: the role of slow kinetics. *Journal of Environmental Quality*, 29, 917-925.

Borisover, M. (2019). Accumulated Gibbs free energy as a quantitative measure of desorption hysteresis associated with the formation of metastable states. *Chemosphere*, 215, 490-499.

Borisover, M. & Graber, E.R. (2002). Simplified link solvation model (LSM) for sorption in natural organic matter. *Langmuir*, 18(12), 4775-4782.

Borisover, M., Sela, M., & Chefetz, B. (2011). Enhancement effect of water associated with natural organic matter (NOM) on organic compound-NOM interactions: A case study with carbamazepine. *Chemosphere*, 82, 1454-1460.

Bowman, B.T. & Sans, W.W. (1985). Partitioning behavior of insecticides in soil-water systems 2. Desorption hysteresis effects. *Journal of Environmental Quality*, 14, 270-273.

Braida, W.J., Pignatello, J.J., Lu, Y.F., Ravikovitch, P.I., Neimark, A.V., & Xing, B.S. (2003). Sorption hysteresis of benzene in charcoal particles. *Environmental Science and Technology*, 37, 409-417.

Cao, X., Lattao, C., Schmidt-Rohr, K., Mao, J. & Pignatello, J.J. (2016). Investigation of sorbate-induced plasticization of Pahokee peat by solid-state NMR spectroscopy. *Journal of Soils & Sediments* 16 (7), 1841-1848.

Chen, X., Meng, Z., Song, Y., Zhang, Q., Ren, L., Guan, L., Ren, Y., Fan, T., Shen, D., & Yang. Y. (2018). Adsorption and desorption behaviors of spirotetramat in various soils and its interaction mechanism. *Journal of Agricultural & Food Chemistry*, 66, 12471−12478.

Fischer, R. & Weiß, H.C. (2008). Spirotetramat (Movento®) – discovery, synthesis and physicochemical properties. *Bayer Crop Science Journal*, 61, 127–140.

Gaonkar, O.D., Nambi, I.M & Govindarajan, S.K. (2019). Soil organic amendments: impacts on sorption of organophosphate pesticides on an alluvial soil. *Journal of Soils & Sediments*, 19, 566–578.

Graber, E.R., Tsechansky, L., & Borisover, M. (2007). Hydration-assisted sorption of a probe organic compound at different peat hydration levels: the Link Solvation Model. *Environmental Science & Technology*, 41, 547-554.

He, Y., Xu, J., Wang, H., Zhang, Q., Muhammad, A. (2006). Potential contributions of clay minerals and organic matter to pentachlorophenol retention in soils. *Chemosphere*, 65, 497-505.

HSDB-Toxnet (2019). Hazardous Substances Data Bank. Imidacloprid CASRN: 138261-41-. https://toxnet.nlm.nih.gov/cgi-bin/sis/search2/f?./temp/~LsfvD4:1 (accessed on 19 November 2019).

Huang, W., Yu, H., & Weber, W.J. (1998). Hysteresis in the sorption and desorption of hydrophobic organic contaminants by soils and sediments. 1. A comparative analysis of experimental protocols. *Journal of Contaminant Hydrology*, 31, 129–148.

IHSS (2019). Acidic functional groups of IHSS substances. http://humic-substances.org/acidic-functional-groups-of-ihss-samples/ (accessed on 19 November 2019).

Jeschke, P. (2016). Propesticides and their use as agrochemicals. *Pest Management Science*, 72, 210-225.

Kandil, M.M., El-Aswad, A.F. & Koskinen, W.C. (2015). Sorption–desorption of imidacloprid onto a lacustrine Egyptian soil and its clay and humic acid fractions. *Journal of Environmental Science & Health, Part B*, 50, 473-483.

Kim, J-H., Gan, J., Farmer, W.J., Yates, S.R., Papiernik, S.K. & Dungan, R.S. (2003). Organic matter effects on phase partition of 1,3-dichloropropene in soil. *Journal of Agricultural Food Chemistry*, 51, 165−169.

Leenheer, J.A., Wershaw, R.L., Brown, G.K., Reddy, M.M. (2003). Characterization and diagenesis of strong-acid carboxyl groups in humic substances. *Applied Geochemistry*, 18, 471-482.

Lu, Y., Pignatello, J.J., 2002. Demonstration of the "conditioning effect" in soil organic matter in support of a pore deformation mechanism for sorption hysteresis. *Environmental Science & Technology. 36*, 4553-4561.

Martins, E.C., Melo, V.d.F., Bohone, J.B. & Abate, G. (2018). Sorption and desorption of atrazine on soils: The effect of different soil fractions. *Geoderma*, 322, 131-139.

Mosquera-Vivas, C.S., Hansen, E.W., García-Santos, G., Obregón-Neira, N., Celis-Ossa, R.E., González-Murillo, C.A., Juraske, R., Hellweg, S. & Guerrero-Dallos, J.A. (2016). The effect of the soil properties on adsorption, single-point desorption, and degradation of chlorpyrifos in two agricultural soil profiles from Colombia. *Soil Science*, 181, 446–456.

OECD (2000). Adsorption - Desorption Using a Batch Equilibrium Method. https://doi.org/10.1787/9789264069602-en (accessed on 19 November 2019).

Oh, S., Wang, Q., Shin, W.S. & Song, D-I. (2013). Effect of salting out on the desorption-resistance of polycyclic aromatic hydrocarbons (PAHs) in coastal sediment. *Chemical Engineering Journal*, 225, 84–92.

Piwowarczyk, A.A. & Holden, N.M. (2012). Adsorption and desorption isotherms of the nonpolar fungicide chlorothalonil in a range of temperate maritime agricultural soils. *Water Air Soil Pollution*, 223, 3975–3985.

Ran, Y., Huang, W., Rao, P.S.C., Liu, D., Sheng, G., & Fu, J. (2002). The role of condensed organic matter in the nonlinear sorption of hydrophobic organic contaminants by a peat and sediments. *Journal of Environmental Quality*, 31, 1953–1962.

Sander, M. & Pignatello, J.J. (2009). Sorption irreversibility of 1,4-dichlorobenzene in two natural organic matter-rich geosorbents. *Environmental Toxicology & Chemistry*, 28 (3), 447-457.

Sander, M., Lu, Y. & Pignatello, J.J. (2005). A thermodynamically based method to quantify true sorption hysteresis. *Journal of Environmental Quality*, 34, 1063-1072.

Wu, W. & Sun, H. (2010). Sorption–desorption hysteresis of phenanthrene – Effect of nanopores, solute concentration, and salinity. *Chemosphere*, 81, 961–967.

Zhang, H., Lin, K., Wang, H. & Gan, J. (2010). Effect of *Pinus radiata* derived biochars on soil sorption and desorption of phenanthrene. *Environmental Pollution*, 158, 2821-2825.

Zhang, W., Ding, Y., Boyd, S.A., Teppen, B.J. & Li, H. (2010). Sorption and desorption of carbamazepine from water by smectite clays. *Chemosphere*, 81, 954-960.

Zhang, X., He, L., Sarmah, A.K., Lin, K., Lin, Y., Li., J. & Wang, H. (2014). Retention and release of diethyl phthalate in biochar-amended vegetable garden soils. *Journal of Soils & Sediments*, 14, 1790–1799.

Zhang, P., Ren, C., Sun, H. & Min, L. (2018). Sorption, desorption and degradation of neonicotinoids in four agricultural soils and their effects on soil microorganisms. *Science of the Total Environment* 615, 59-69.